Observation of a Stationary, Current-Free Double Layer in a Plasma

G. Hairapetian and R. L. Stenzel

Department of Physics, University of California at Los Angeles, Los Angeles, California 90024-1547

A stationary, current-free, potential double layer is formed in a two-electron-population plasma due to self-consistent separation of the two electron species. The position and amplitude of the double layer are controlled by the relative densities of the two electron populations. The steady-state double layer traps the colder electrons on the high potential side, and generates a neutralized, monoenergetic ion beam on the low potential side. The field-aligned double layer is annihilated when an electron current is drawn through the plasma.

Potential double layers[1] are localized electrostatic potential structures created by two equal but opposite space-charge layers, which are capable of sustaining high potential drops in collisionless plasmas. Double layers are highly nonlinear structures, and are thought to be responsible for particle acceleration in laboratory[2] plasmas, aurora,[3] and solar flares.[4] They have been generated in laboratory experiments[2] by various methods such as ionization processes, injection of electron and ion beams, driving a current through plasma, and applying a potential difference between two plasmas. Most laboratory double layers require the presence of a relative electron-ion drift (i.e., a plasma current). In most cases, the drift velocity exceeds the electron thermal velocity; however, double layers with $v_d < v_{et}$ have also been observed.[5] Steady-state, currentless[6] ($v_d \ll v_{et}$ or $v_d \simeq 0$) double layers, on the other hand, are rarely observed except in the vicinity of strong magnetic-field gradients.[7] In this Letter, the observation of a stationary, currentless double layer in a collisionless, uniformly magnetized plasma is described.

The experiment is performed in a large, high-vacuum chamber (80-cm diameter, 170-cm length, $P_0 \simeq 2 \times 10^{-7}$ Torr). The discharge plasma is generated locally by ionizing a pulsed ($t_{on} = 1$ ms, $t_{off} = 3$ s), collimated neutral (Ar) beam that is injected radially by a piezoelectric leak valve into a filamentary cathode. The cathode heater is pulsed so as to emit monoenergetic primary electrons. In the vicinity of the cathode, the neutral beam has a density of 1.6×10^{13} cm^{-3} ($P = 5 \times 10^{-4}$ Torr), and is quickly ionized ($t < 7$ μs) by the primary electrons ($V_{dis} = 80$ V, $I_{dis} = 4$–10 A). With continuous pumping, the background neutral pressure is maintained at below 2×10^{-6} Torr. The pulsed discharge plasma ($n_e \simeq 10^{11}$ cm^{-3}, $kT_e \simeq 4$ eV, $T_i \lesssim 0.5$ eV) expands[8] supersonically [$v_{flow} > C_s \simeq 3.1 \times 10^5$ cm/s, where $C_s = (kT_e/M)^{1/2}$, $kT_e \simeq 4$ eV] along a uniform axial magnetic field ($B_z = 30$–50 G), and reaches the end of the chamber in $t \lesssim 100$ μs. The electron population at the source consists of a cold, high-density Maxwellian ($n_M \simeq 10^{11}$ cm^{-3}, $kT_e \simeq 4$ eV) and a low-density tail

($\frac{1}{2} mv^2 \simeq eV_{dis} \simeq 80$ eV, $n_{tail}/n_M \simeq 0.03$) with an isotropic shell distribution. The ratio of n_{tail} to n_M is controlled by varying the density of the injected neutral gas while maintaining a constant discharge current. As the neutral density is increased, due to increased ionization in the source, the densities of secondary (Maxwellian) electrons and ions increases (i.e., n_{tail}/n_M decreases). Figure 1 shows schematically the experimental setup along with the steady-state plasma potential profile on the central axis of the device. The cathode is grounded to maintain a constant anode potential ($+80$ V) with respect to the chamber wall (ground). Most of the discharge current ($\geq 98\%$) flows from the grounded cathode to the anode (separation $\simeq 0.5$ cm) while the rest ($\leq 2\%$) flows to the grounded end plate through the plasma. The axial magnetic field confines the electrons radially ($r_l \simeq 0.5$ cm) and produces a high-density plasma column (12 cm diam), well separated from the chamber wall (80 cm diam). Because of the strong axial density gradient ($n/\nabla n \simeq 3$ cm) of the injected gas, ionizing and charge-exchange collisions are restricted to the vicinity of the source. This condition is critical for the formation of the double layer, as no double layer is observed at high background pressures ($p > 2 \times 10^{-5}$ Torr). The double layer and associated processes are studied with emissive probes, directional velocity analyzers,[9] Langmuir probes, and microwave resonator probes.[10]
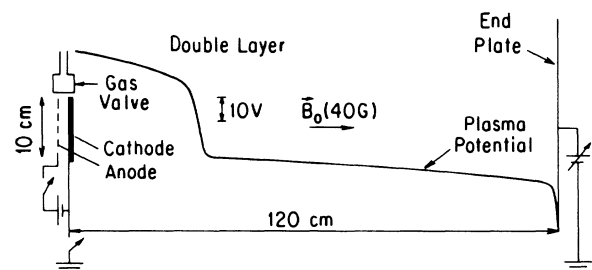

FIG. 1. Schematic side view of the experimental device (not to scale), along with the plasma potential profile on the central axis of the device.
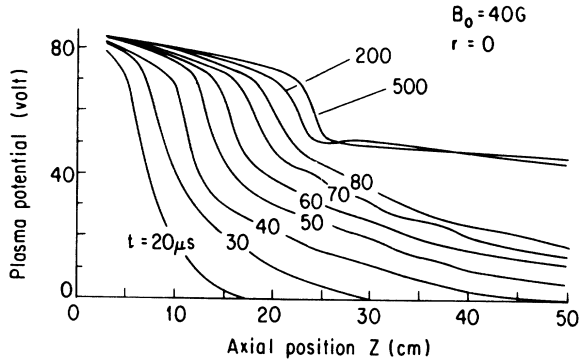
FIG. 2. Measured temporal evolution of the plasma potential profiles along the axis. $z = 0$ corresponds to the position of the source; and $t = 0$, to the turnon of the discharge pulse.

FIG. 3. (a) Contours of constant plasma potentials ($\Delta\phi = 3$ V between contours) showing the steady-state double layer at $t = 500$ μs. (b) The radial plasma density profile (arbitrary units).

The plasma potential profile is probed with a fast (response time ≤ 0.5 μs) emissive probe (0.1 mm diam, 3 mm long) heated by a pulsed dc power supply. The floating potential of the emissive probe is measured with a fast buffer, mounted on the probe shaft inside the chamber. At each spatial position, the floating potential of the emissive probe as a function time is averaged over ten shots, and stored for processing in a computer. Figure 2 shows the evolution of the plasma potential profiles measured at 1-cm spatial increments along the axis. As a function of time, the potential profile broadens and develops a well-defined "knee" (a double layer). Most of the electrostatic field remains localized within this double layer, which propagates away from the source at decreasing velocity ($v \leq C_s$) and amplitude. At $t \geq 200$ μs, the double layer [$\Delta\phi \simeq 20$–60 V, $\Delta z \simeq 2.5$–5 cm $\simeq (50$–$100)\lambda_D$] reaches a steady state and stagnates. Although the double layer undergoes some further evolution due to changes in the source, it maintains its steady-state conditions till the end of the discharge ($\Delta t \simeq 1$ ms). After the discharge is switched off, the double layer decays in less than 10 μs.

Two-dimensional (z and r) potential profiles are mapped over a half plane of 30×75 cm^2 containing 286 spatial points. Figure 3 shows (a) contours of constant plasma potential and (b) the radial plasma density profile at $t = 500$ μs. Most of the electric field is concentrated at the double layer, and the electric field within the double layer is mainly parallel to the ambient magnetic field. With the magnetic field off, the double layer still forms; however, on the low potential side, the radial electric field at the edge of plasma column reverses direction. The position where the double layer stagnates ($z \simeq 15$–40 cm) and its amplitude ($\Delta\phi \simeq 20$–60 V) are determined by the relative densities of the two electron species in the source.

The ions are accelerated by the double layer to form a low-density, high-energy beam. Upon impact with the end plate, the ions are neutralized. The parallel ion dis-
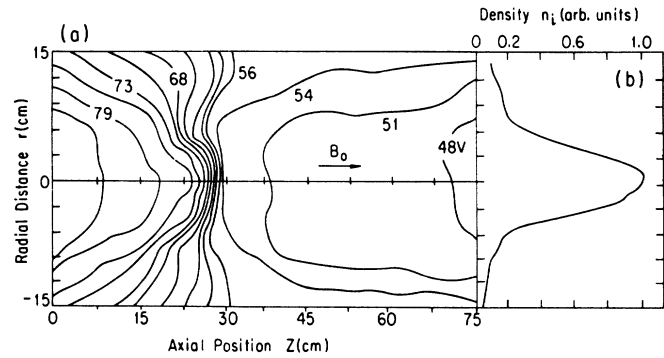
tribution function is measured with a directional retarding-grid energy analyzer (energy resolution $= 0.5$ eV). The directional energy analyzer with a small angular resolution ($\Delta\theta \simeq 6°$) measures the true velocity-space distribution function. Near the source ($z < 5$ cm), only cold ($kT_i < 1$ eV) ions are observed. Away from the source, the ions are accelerated to supersonic velocities ($v > C_s$) before entering the double layer. When the ions traverse the double layer, they are further accelerated by the strong, localized electric field. On the low potential side, the ions have a beamlike distribution function with a small velocity spread ($kT_b \simeq 0.1$ eV), and a narrow angular divergence ($\Delta\theta \simeq 12°$). The kinetic energy of the ions is equal to the potential drop across the double layer, and no stationary ion population is present.

The relative electron densities are measured with a small Langmuir probe (3 mm diam); and the absolute densities, with the microwave resonator probe (axial resolution $\simeq 2$ mm). Because of the high density of plasma, the inferred space-charge imbalance is limited to $(n_e - n_i)/n_e \leq 0.002$, which is beyond the resolution of probes. Figure 4 shows (a) the steady-state plasma potential and (b) the corresponding density profiles along the central axis for different values of n_{tail}/n_M. The plasma density decreases exponentially (linearly on the vertical log scale) away from the source. The density gradient, which is strongest (40% per cm) at the double layer, is mainly due to reflection of the electrons and acceleration of ions by the space-charge electric field. By plotting the plasma potential versus the logarithm of electron density, one can estimate the parallel temperature of the electrons from the slope of the curve, $e\phi = kT_e \ln(n/n_0)$ (Boltzmann's relation). The estimated temperature for the electrons on the high potential side is about 3.5 eV which agrees well with $kT_e \simeq 4$ eV as measured with a Langmuir probe. At the double layer, the effective parallel electron temperature is about 29 eV which compares well with the expected value of 27 eV (since the energetic electrons have an isotropic distri-
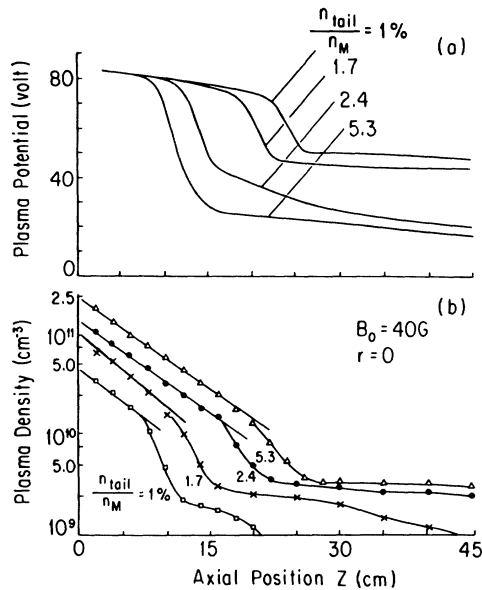
FIG. 4. (a) Steady-state plasma potential profiles along the axis for different values of n_{tail}/n_M at the source. (b) The corresponding plasma density profiles [log(n) vs Z].

bution, the average parallel energy is $\frac{1}{3}$ of total energy $\simeq 80$ eV). The potential drop ($\Delta\phi \simeq 20$-50 V) at the double layer is of the order of the "free" electron temperature ($\simeq 29$ eV); hence, this is a weak double layer. At the source, the Maxwellian electrons dominate ($n_{\text{tail}}/n_M \leq 0.05$). As the distance from the source increases, the Maxwellian electrons are retarded; n_M decreases and n_{tail}/n_M increases as confirmed by Langmuir-probe measurements. Finally, the energetic electrons dominate the electron population. The double layer forms at a position where the transition in electron population occurs ($n_{\text{tail}} \geq n_M$), as predicted by earlier theoretical and computer simulation studies.[11] Obviously, the higher the density of Maxwellian electrons, the farther away from the source the transition would occur; this is why the position of the double layer is controlled by the relative densities of the two electron species. Because of changes in the neutral gas density as a function of time, n_{tail}/n_M changes over time. These variations in the density are reflected in the late ($t > 200$ μs) evolution of the double layer. During the density increase the steady-state double layer moves farther away from the source ($\Delta z \simeq 2$ cm, $\Delta t \simeq 300$ μs); and during the decrease, it returns toward the source ($\Delta z \simeq -4$ cm, $\Delta t \simeq 500$ μs).

The low potential region consists of a steady-state, monoenergetic ion beam and retarded energetic electrons which were able to overcome the double-layer potential ($\frac{1}{2}mv_{\parallel}^2 \geq e\Delta\phi$). The retarded electrons are reflected by the grounded end plate and are accelerated back toward the source by the double layer. The electron distribution function is isotropic with a broad velocity spread

($\frac{1}{2}m\bar{v}^2 \simeq 10$-15 eV) as measured with the directional analyzer. A small net current (of the order of ion saturation current) flows through the plasma. When the net current through the plasma is reduced to zero by floating the anode-cathode structure, no significant changes (to within 10%) are observed in the position, amplitude, or width of the double layer even though the absolute value of potential with respect to the chamber wall changes. In contrast, when the end plate is biased positively with respect to the cathode to draw electron current, the double-layer amplitude decreases and finally disappears as the bias voltage is increased. The positively biased end plate collects the retarded electrons and reduces the excess negative space charge. As expected, a negative bias has no effect on the double layer. The double-layer amplitude depends on the ratio n_{tail}/n_M. When n_{tail}/n_M decreases due to an increase in densities of secondary electrons and ions, the ion flux into the low potential region increases. The additional ions neutralize some of the negative space charge and thereby reduce the amplitude of the potential drop. Conversely, when n_{tail}/n_M increases, the ion flux is reduced and the double layer becomes stronger.

In summary, we have investigated the formation of a stationary, current-free, double layer in a two-electron-population plasma. The necessary conditions for the formation of the double layer are existence of two electron species with different "effective" temperatures, a mechanism for electrostatic trapping of the hotter electrons, and the absence of any ionizing or charge-exchange collisions. The weak double layer forms due to self-consistent separation of the two electron species. The final position and amplitude of the double layer are determined by the relative densities of the two electron populations in the source. The double layer contains no trapped or counterstreaming ion population, no electron beams, and hence, no sources for microinstabilities. It traps the cold Maxwellian electrons in the high potential side, retards the energetic electrons, and accelerates ions. These laboratory observations have significant implications on ion-acceleration and electron-trapping mechanisms in space (e.g., AMPTE and critical ionization velocity experiments) and laser plasmas. Fast ions are not only produced during the transient expansion process but also in steady state by the described double layer in the two-electron-population plasmas.

[1]L. P. Block, Astrophys. Space Sci. 55, 59 (1978).
[2]For a review of laboratory experiments see the following papers: S. Torvén, in Wave Instabilities in Space Plasmas, edit-

ed by P. J. Palmadesso and K. Papadopoulos (Reidel, Dordecht, 1979), Vol. 74, p. 109; N. Sato, in *Proceedings of the Symposium on Plasma Double Layers,* edited by P. Michelsen and J. Juul Rasmussen (Risø National Laboratory, Roskilde, Denmark, 1982), p. 116.

[3]H. Alfvén, Tellus **10**, 104 (1958); Wescott *et al.*, J. Geophys. Res. **81**, 4495 (1976); F. S. Mozer *et al.*, Phys. Rev. Lett. **38**, 292 (1977).

[4]H. Alfvén and P. Carlqvist, Sol. Phys. **1**, 220 (1967).

[5]Ch. Hollenstein *et al.*, Phys. Rev. Lett. **45**, 2110 (1980); C. Chan *et al.*, Phys. Rev. Lett. **57**, 3050 (1986).

[6]D. P. Stern, J. Geophys. Res. **86**, 5839 (1981); F. W. Perkins and Y. C. Sun, Phys. Rev. Lett. **46**, 115 (1981).

[7]R. Hatakeyama *et al.*, Phys. Rev. Lett. **50**, 1203 (1983); Y. Nakamura and R. L. Stenzel, in *Proceedings of the Symposium on Plasma Double Layers* (Ref. 2), p. 153.

[8]G. Hairapetian and R. L. Stenzel, Phys. Rev. Lett. **61**, 1607 (1988).

[9]R. L. Stenzel *et al.*, Rev. Sci. Instrum. **53**, 59 (1982).

[10]R. L. Stenzel, Rev. Sci. Instrum. **47**, 603 (1976).

[11]L. M. Wickens *et al.*, Phys. Rev. Lett. **41**, 243 (1978); B. Bezzerides *et al.*, Phys. Fluids **21**, 2179 (1978); J. Denavit, Phys. Fluids **22**, 1384 (1979); M. A. True *et al.*, Phys. Fluids **24**, 1885 (1981).